Trap loss in a two-species Rb-Cs magneto-optical trap

G. D. Telles, W. Garcia, L. G. Marcassa, and V. S. Bagnato
Instituto de Física de São Carlos, Universidade de São Paulo, Caixa Postal 369, 13560-970, São Carlos-SP, Brazil

D. Ciampini, M. Fazzi, J. H. Müller, D. Wilkowski,* and E. Arimondo
Istituto Nazionale per la Fisica della Materia and Dipartimento di Fisica, Università di Pisa, Via F. Buonarroti 2, I-56126 Pisa, Italy
(Received 14 June 2000; published 14 February 2001)

We investigate inelastic cold collisions in a Rb-Cs mixed-species trap where the rubidium trap loss rate was measured. We present the experimental results and a qualitative discussion for the observation. These studies are relevant for high-resolution atomic and molecular spectroscopy, and for the production of mixed-species Bose-Einstein condensates.

DOI: 10.1103/PhysRevA.63.033406 PACS number(s): 32.80.Pj, 33.80.Ps, 34.50.Rk, 34.80.Qb

I. INTRODUCTION

During the past years, many experiments have been devoted to the study of excited-ground-state cold collisions using a sample of trapped cold atoms [1,2]. Recently, there has been greater interest in the study of collision mechanisms involving two different kinds of atoms in a mixed-species magneto-optical trap (MOT) [3–9]. The nature of these collisions bears critically on matter-wave coherence and quantum-statistical condensates of a dilute sample cloud of atoms.

Concerning the homonuclear alkali-metal collision mechanisms, particular interest has been drawn to the inelastic processes that lead to atom losses from the MOT. It is well established that the main process causing those losses is radiative escape (RE), as described in a recent review [2]. Other mechanisms may contribute to the trap losses, for instance fine-structure change (FSC), with a loss rate between a few percent and 30% of the total loss rate, depending on the atomic species [10–12]. In the low-intensity regime, the hyperfine change collision (HCC) becomes also an important mechanism for losses [2].

For heteronuclear cold collisions the loss mechanisms are the same ones. However, the internuclear long-range potential is weaker and the shorter-range interactions are more important. The dominant interaction term for the homonuclear ground-excited collisions depends on R^{-3}, while for heteronuclear collisions it depends on R^{-6} [13], with R the internuclear distance. Thus the colliding atoms have to get much closer for the above-mentioned loss processes effectively to take place. Therefore the probabilities of those mechanisms are considerably modified and within the laser-cooling community it is important to identify and to understand the main physical processes involved in the two-species systems. Furthermore, the results obtained on two-species losses will be important for the development of sympathetic cooling between rubidium and cesium, and for the realization of other two-species quantum systems [14].

In the present investigation we have chosen the Rb-Cs combination for a study of the two-species trap losses because of the large Franck-Condon factor value recently predicted for this atomic combination [15]. This means that this heteronuclear system will provide a large number of ground-excited quasimolecule pairs, and it will be particularly convenient for performing photoassociative spectroscopy experiments.

The Rb-Cs trap losses have been measured in two separate experiments, the first one by the Brazilian group and the second one by the Italian group. There are two important differences between these experiments. In the Brazilian experiment the trap rate was investigated for ^{85}Rb in an intensity range from 40 to 250 mW/cm^2 and in the Italian experiment the ^{87}Rb trap loss was investigated from 10 to 45 mW/cm^2. In both cases the rubidium atoms collide with ^{133}Cs atoms. The difference in the hyperfine structures of the two rubidium isotopes may play a subtle role in the Rb-Cs cold collisions, but the present comparison between the experimental results by the two separate experiments does not show any pronounced difference. The setups in the two experiments are compared in Sec. II. The similar data analysis of the loss rates is presented in Sec. III. The comparison between results and their discussion are in Sec. IV.

II. EXPERIMENTAL SETUP

The Brazilian experiment was based on a closed stainless-steel vapor cell, containing four different reservoirs for sodium, potassium, rubidium, and cesium atoms [6]. Controlling the temperature of the reservoirs and the opening of input valves allowed to choose the species to be trapped. The Italian experiment operates in a quartz cell, containing in a side stainless-steel chamber alkali-metal dispensers producing the cesium and rubidium background atoms. The individual flux of both species was finely controlled through the current of the dispensers.

The Brazilian experiment used two Ti:sapphire (Coherent 899) lasers, generating the trapping frequencies for both rubidium and cesium, and two stabilized diode lasers to provide the repumping transition frequencies. The detunings of trap lasers $\Delta_{T,\mathrm{Rb}}$ and $\Delta_{T,\mathrm{Cs}}$, respectively, are specified in Table I in units of the linewidths Γ_{Rb} and Γ_{Cs} for the atomic transitions. In the *xy* plane there are two independent counterpropagating laser beams entering the vapor cell for each

*Permanent address: Université de Nice, INLN, 1361 route de Lucioles, F-06560 Valbonne, France.

TABLE I. MOT parameters and typical values in the Brazilian and Italian experiments.

Parameter	Brazilian experiment	Italian experiment
Colliding species	^{85}Rb-^{133}Cs	^{87}Rb-^{133}Cs
Rb cooling transition	$5S_{1/2}(F=3)\Rightarrow 5P_{3/2}(F'=4)$	$5S_{1/2}(F=2)\Rightarrow 5P_{3/2}(F'=3)$
Cs cooling transition	$5S_{1/2}(F=4)\Rightarrow 5P_{3/2}(F'=5)$	$5S_{1/2}(F=4)\Rightarrow 5P_{3/2}(F'=5)$
$\Delta_{T,\mathrm{Rb}}$	$-0.8\Gamma_{\mathrm{Rb}}$	$-1.4\Gamma_{\mathrm{Rb}}$
$\Delta_{T,\mathrm{Cs}}$	$-1.3\Gamma_{\mathrm{Cs}}$	$-2.0\Gamma_{\mathrm{Cs}}$
$I_{\mathrm{tot}}^{\mathrm{Rb}}$	40–250 mW/cm^2	10–45 mW/cm^2
$I_{\mathrm{tot}}^{\mathrm{Cs}}$	400 mW/cm^2	40 mW/cm^2
N_{Rb}	10^8	2×10^6
N_{Cs}	10^8	5×10^6
n_{Rb}	2×10^{10} cm^{-3}	1.5×10^{10} cm^{-3}
n_{Cs}	8×10^9 cm^{-3}	7.2×10^9 cm^{-3}

species. In the z axis the Rb and Cs laser beams are combined in a dichroic mirror. Circular polarized light in the xy plane is produced by $\lambda/4$ plates for each species and by Fresnel rhombs in the z axis. This scheme of independent optics for each atomic species guaranteed very good control of the spatial overlap for the two trapped atomic clouds. The trap laser was operated at about six times more power than the repumper. The number of trapped atoms of both species were determined by imaging their fluorescence onto a calibrated photomultiplier tube (PMT), while their dimensions were measured with a charge-coupled device camera (CCD) and passband optical filters. The atomic densities were obtained using these parameters.

The Italian experiment was based on diode lasers assembled in a master-slave configuration, the rubidium cooling slave laser being a tapered amplifier with 300-mW output and the cesium cooling laser a 200-mW diode laser. Radiation from both cooling lasers was combined within a single-mode optical fiber, with 65% transmission at both wavelengths. All the optical components at the fiber output required for the laser cooling of the two species operated at both 780 and 850 nm wavelengths. A fine tuning in the final position of the Rb and Cs cold clouds was realized by inserting additional quarter-wave plates in order to control independently the circular polarization of Rb and Cs cooling lasers. The detunings of the trap lasers for both atomic species and the cesium total cooling laser intensity $I_{\mathrm{tot}}^{\mathrm{Cs}}$ are listed in Table I. The fluorescence of each trapped atomic species was measured using narrow-band interference filters and calibrated photomultiplier or photodiodes. It was verified that the transmittance of each interference filters at the other wavelengths produced a negligible influence on the measured quantities. Cold cloud sizes and shapes were measured with CCD cameras. The number of atoms was derived from the fluorescence intensities measured for each species. For both Rb and Cs and for all the trap laser intensities, the CCD camera images of the cold atom clouds assured the spatial distributions to be very close to Gaussian ones.

In both experiments the MOT parameters (magnetic gradient, laser beam waist) were chosen in order to produce a Gaussian waist [16] of the Rb cloud smaller than that of the Cs cloud, $w_{\mathrm{Rb}}\sim 1$ mm and $w_{\mathrm{Cs}}\sim 1.5$ mm for the Brazilian experiment, and $w_{\mathrm{Rb}}\sim 0.3$ mm and $w_{\mathrm{Cs}}\sim 0.6$ mm, respectively for the Italian experiment. Individual trapped densities and total numbers of atoms in the two experiments are listed in Table I. The listed total number of atoms and their density presented there for each species represent values in the absence of the other species.

III. DETERMINATION OF THE CROSS-SPECIES TRAP LOSS RATE

The trap loss rate was determined from the analysis of the trap loading or unloading signal acquired by either a PMT or photodiode device following a switch on/off sequence of the trapping lasers beams. We examined the rubidium trap in the presence and the absence of the Cs sample. In this configuration, the following rate equation describes the temporal evolution of the number N_{Rb} atoms in the trap:

$$\frac{dN_{\mathrm{Rb}}}{dt}=L-\gamma N_{\mathrm{Rb}}-\beta\int_V n_{\mathrm{Rb}}^2 d^3r-\beta'\int_V n_{\mathrm{Rb}}n_{\mathrm{Cs}}d^3r, \quad (1)$$

where L is the loading rate, γ is the loss rate caused by collisions between the trapped Rb atoms and the hot background gas (composed mainly of thermal Rb and Cs), β is the loss rate resulting from collisions among the trapped rubidium atoms, and β' is the Rb loss rate due to cold collisions with trapped cesium atoms, n_{Rb} and n_{Cs} are the density profiles of rubidium and cesium atoms, and N_{Rb} is the number of trapped rubidium atoms. We have to emphasize that β' should be read as $\beta'_{\mathrm{Rb\text{-}Cs}}$, unless mentioned; also, the subindex arrangement Rb-Cs indicates that the first species, Rb in this case, is the one in which increased losses are observed when the second species, Cs in this case, is present. The integration in Eq. (1) is calculated over the whole volume occupied by the Rb atoms.

It is important to mention that if we had chosen to study the Cs atoms instead of Rb, Eq. (1) would be identical, except for the Cs subindexes. However, there should be no reason for $\beta'_{\mathrm{Cs\text{-}Rb}}$ to be reciprocal to $\beta'_{\mathrm{Rb\text{-}Cs}}$, the extra loss rate coefficient for the Rb sample. The lack of reciprocity is readily justified considering, for example, that the different C_6 coefficients involved in all possible collision channels in

each situation are different. Moreover, the trap depths for the two MOT's are not equal and they may change in different ways with the other MOT parameters during the experiments.

For Gaussian spatial atomic distributions, $n_{\mathrm{Rb}}(r,t) = n_0^{\mathrm{Rb}}(t)e^{-2(r/w_{\mathrm{Rb}})^2}$ and $n_{\mathrm{Cs}}(r,t) = n_0^{\mathrm{Cs}}(t)e^{-2(r/w_{\mathrm{Cs}})^2}$, Eq. (1) becomes

$$\frac{dN_{\mathrm{Rb}}}{dt} = L - \left\{ \gamma + \beta' N_{\mathrm{Cs}} \left[\frac{2}{\pi(w_{\mathrm{Rb}}^2 + w_{\mathrm{Cs}}^2)} \right]^{3/2} \right\} \times N_{\mathrm{Rb}} - \beta \left(\frac{1}{\pi w_{\mathrm{Rb}}^2} \right)^{3/2} N_{\mathrm{Rb}}^2. \tag{2}$$

Notice that the cloud widths w_{Rb} and w_{Cs} are implicit functions of time as the clouds grow during loading in the constant density regime. This form of Eq. (2) will be useful, however, when extracting the interspecies loss coefficient β' from steady-state data.

In the Brazilian experiment the approach applied to derive the loss coefficient relied on the determination of the steady-state values for the rubidium atoms, in the absence and presence of Cs. In the absence of Cs, the observation of $N_{\mathrm{Rb}}(t)$ and its mathematical fitting with the solution of Eq. (2) allowed the determination of β and γ. From the steady-state values for the rubidium atoms, in the absence and presence of Cs, we can obtain β'. We denote N_{Rb} the number of the rubidium atoms in the MOT and w_{Rb} its width in absence of cesium, while the N_{Rb}^* and w_{Rb}^* are the corresponding number and waist in the presence of N_{Cs} atoms. The steady-state solution of Eq. (2) in the absence and presence of Cs atoms leads to the following relation for β':

$$\beta' = \left[\frac{\pi(w_{\mathrm{Rb}}^2 + w_{\mathrm{Cs}}^2)}{2} \right]^{3/2} \frac{1}{N_{\mathrm{Cs}} N_{\mathrm{Rb}}^*} \left\{ \gamma(N_{\mathrm{Rb}}^* - N_{\mathrm{Rb}}) + \beta \left[\left(\frac{1}{\pi w_{\mathrm{Rb}}^{*2}} \right)^{3/2} N_{\mathrm{Rb}}^* - \left(\frac{1}{\pi w_{\mathrm{Rb}}^2} \right)^{3/2} N_{\mathrm{Rb}} \right] \right\}. \tag{3}$$

The β' determination based on this formula will be denoted as the steady-state approach.

For the Italian experiment, the system is operated in the density-limited regime and the rubidium cloud was immersed into the region of the cesium cloud where its density could be assumed constant; in this case, Eq. (2) may be written as

$$\frac{dN_{\mathrm{Rb}}}{dt} = L - \gamma N_{\mathrm{Rb}} - \beta' n_{\mathrm{Cs}} N_{\mathrm{Rb}} - \beta f(N_{\mathrm{Rb}}) n_{\mathrm{Rb}} N_{\mathrm{Rb}} = L - R_P N_{\mathrm{Rb}}, \tag{4}$$

where the exponential rate R_P for the Rb loading has been introduced

$$R_P = \gamma + \beta' n_{\mathrm{Cs}} + \beta f(N_{\mathrm{Rb}}) n_{\mathrm{Rb}}, \tag{5}$$

with the factor $f(N_{\mathrm{Rb}})$ accounting for the deviation of the Rb cloud-density distribution from the uniform density n_{Rb} value [17]. The exponential loading rate R_P of the trap, and its dependence on the Cs density given by Eq. (5), was measured. Such a technique, to be denoted in the following as the loading method, represents the standard one for the determination of the cold collision rates.

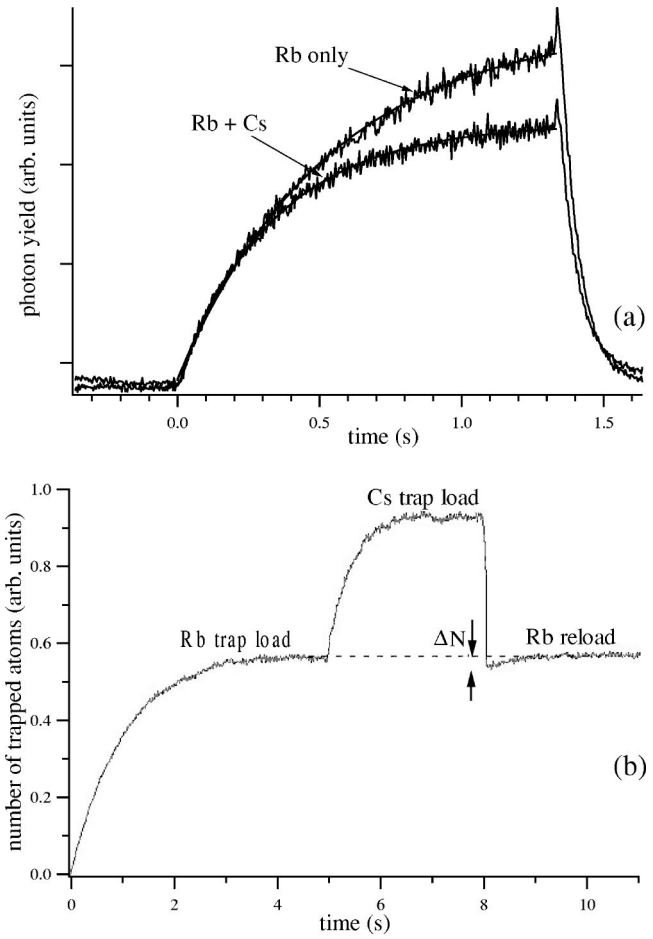

FIG. 1. (a) Typical loading curves of the Rb MOT recorded by a photodiode in the Italian experiment in the absence and presence of cold Cs atoms. (b) Typical fluorescence time dependence recorded in the Brazilian experiment during the sequence described in the text for loading the Rb and Cs MOTs. The signal proportional to $\Delta N = N_{\mathrm{Rb}}^* - N_{\mathrm{Rb}}$ has been marked. MOT parameters listed in Table I.

In the Italian experiment, where the loading approach was applied to derive β', the cold cloud image on calibrated photodiodes allowed us to record the time dependence of the emitted atomic fluorescence. The transient loading curve for the each species MOT was recorded, blocking the Cs or Rb repumper light, respectively, while leaving the trap lasers always on. An example of the Rb loading in the absence of Cs is shown in Fig. 1(a). The number of N_{Rb} and N_{Cs} atoms in the absence of the other species was derived from those fluorescence records. In a second step, in which the Rb trap was formed in the presence of the Cs MOT, the calibrated photodiode recorded the loading curve of the Rb trap, as shown also in Fig. 1(a). With Cs introduced, a reduction of as much as 30% was observed in the total number of trapped Rb atoms. The number of rubidium atoms was extracted from the fluorescence signal, even if the β' determination did

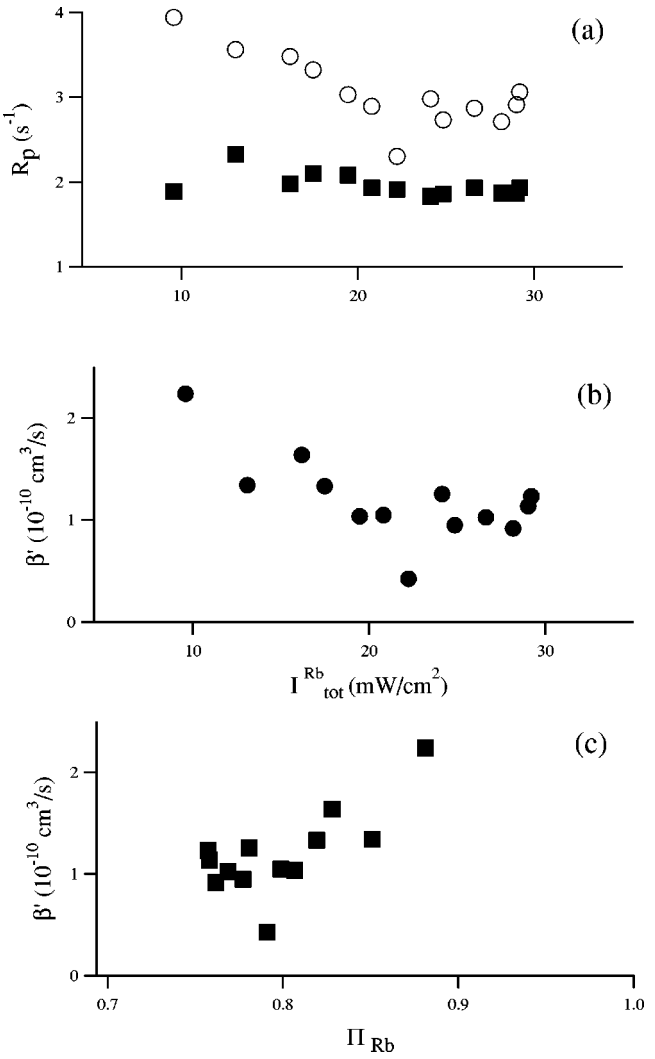

FIG. 2. Experimental results for the Rb losses produced by collisions with Cs in the Italian experiment. In (a) MOT loading rate R_P in units of s^{-1}, vs the trap laser total intensity I_{tot}^{Rb}, with closed squares for the case of Rb only, and open circles when simultaneous Cs cooling took place. In (b) β' values, in units of $10^{-10}\,cm^3\,s^{-1}$, derived from the data in (a) using the n_{Cs} value of Table I. In (c) β' values versus ground-state occupation Π_{Rb}, modified by the Rb trap laser intensity. Note that Π_{Rb} increases with decreasing I_{tot}^{Rb}.

not require the N_{Rb} value. The fit of the loading curves by the exponential loading of Eqs. (4) and (5) determined R_P. Experimental results for R_P versus the total intensity I_{tot}^{Rb} of the Rb trap lasers are shown in Fig. 2(a) for both cases of Rb only and Rb in presence of Cs atoms. Using the definition of Eq. (5), the difference between these exponential rates gives the additional loss term $\beta' n_{Cs}$ due to heteronuclear collisions. The value of β' was derived from the measurement of the density of cesium atoms, n_{Cs}. The loading measurements reported here suffered from the long-term variations of trap conditions, explicitly avoided in the steady-state procedure applied in the Brazilian experiment. However, it was verified that repeating the measurements of the Rb trap in random sequences with respect to the absence or presence of Cs atoms, consistent values for β' were obtained. As an additional check, the MOT loading was used to measure the β values and to verify their good agreement with those presented in Ref. [18].

The steady-state technique applied in the Brazilian experiment consisted of three steps. The experiment began by blocking one laser beam of each MOT to prevent any kind of species from being trapped. The rubidium laser beam was then unblocked. By imaging the rubidium cloud fluorescence onto the calibrated photomultiplier, the transient loading curve and the steady-state number for the trapped rubidium atoms were determined. When the rubidium MOT reached its steady-state number, its volume was derived from an image taken with a CCD camera. In the second step, the Cs trap was allowed to form, and the loading process was monitored by the same photomultiplier used to observe the Rb fluorescence. When the steady state of the Cs trap was reached, a new CCD image of the overlapped samples was recorded. In the following, the Cs MOT was suddenly emptied by blocking the trap light, and the number of trapped Rb atoms was determined through the variation of the PMT signal. At that point, a new CCD picture of the remaining Rb trap was taken. This procedure defined both the total number of trapped rubidium atoms and the dimensions of the sample with cold cesium present. The CCD recording process took under 3 ms, a time insufficient for the rubidium cloud to change, thus preserving the rubidium cloud shape and number assumed in the presence of Cs. As a final step, the recovery of the number and density of rubidium atoms in the MOT was checked to ensure stability throughout the recording procedure, verifying the full recovery of the initial values. Figure 1(b) shows a typical fluorescence spectrum during the entire sequence described above. When Cs was introduced, a reduction of as much as 10% was observed in the total number of trapped Rb atoms. The β' value was derived from the above procedure making use of Eq. (3). The reduction in fluorescence determined that the number of trapped Rb atoms in the steady state as well as the number of trapped rubidium atoms in the presence of cold cesium decreased relatively to the initial number. The dimensions of the rubidium and cesium samples were derived from sample images framed during the entire procedure and a digital subtraction. The β' values have also been derived applying the loading approach, i.e., through records of the loading process of one species in the presence and absence of the second species using optical filters, as in previously reported work [6], and as performed in the Italian experiment. However, the Brazilian group observed that the data obtained by the steady-state technique varied considerably less in comparison to those derived from the loading rates, mainly because a shorter time was required for data acquisition. Hence, this technique is less sensitive to long-term variations of trap conditions.

We have not included the error bars on the plots for R_P and β' in Figs. 2 and 3 in order to keep the different data sets as clear as possible. Nevertheless, the existence of two points for each intensity in the Brazilian experiment, Fig. 3, shows that the statistical uncertainties are around 30%. Fur-

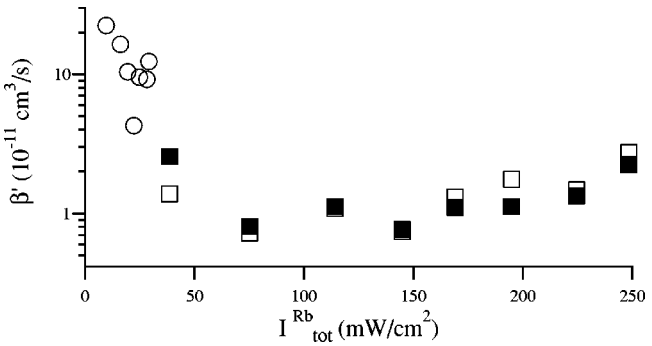

FIG. 3. Rubidium trap laser intensity dependence of β' for Rb in the presence of Cs. The open and closed squares refer to the two different data sets from the Brazilian experiment, while the hollow circles report the data from the Italian experiment, a part of those plotted in Fig. 2(b). This figure has to be examined with care, remembering that the two experiments were performed in different conditions. We have not included error bars to avoid congestion of the plot. A typical 20% uncertainty is associated to the β' measurements, as estimated from the scattering of the data in the Brazilian experiment.

thermore, it has to be mentioned that those were mainly due to errors in the volume measurements of the trapped atomic species.

IV. RESULTS AND DISCUSSION

Figure 3 reports the measured values for the Rb loss rate due to heteronuclear collisions with Cs, β' ($\beta'_{\text{Rb-Cs}}$), versus the rubidium trap laser intensity $I_{\text{tot}}^{\text{Rb}}$ for both experiments. The hollow and solid squares refer to two different data sets for the ^{85}Rb from the B experiment, while the solid circles refer to the ^{87}Rb data from the Italian experiment. Notice that the two data sets from the B experiment were derived from the loading rate and steady-state approaches and they have produced similar β' values. We have to point out that Fig. 3 has to be carefully examined, observing that both experiments have been performed in different experimental conditions. The observed overall behavior of β' with the Rb trap laser intensity does not differ a lot from the β traditionally observed: an increase of β' is observed at both ends of the intensity axis scale. Nevertheless, a comparison between β and β' should always be done with care, once different mechanisms of atomic losses could be involved.

Notice that the Rb-Cs β' values are higher up to two orders of magnitudes than the Rb-Rb β values, for instance the accurate measurements reported in [18]. One contribution to this large value arises from the mass ratio effect: since the Rb mass is smaller than the Cs ($m_{\text{Rb}}/m_{\text{Cs}} \simeq 0.64$), at the end of the collision loss process the energy sharing produces lighter atoms with greater kinetic energies. Therefore the surplus of energy compared to the trap potential depth induces higher trap loss rates for the lighter atom, rubidium in this case, with 62% of the released energy picked up. The larger values expected for the lighter species represents the main reason why in the present investigations attention was concentrated on rubidium. The Brazilian experiment has also measured the effect of Rb on the Cs trap, obtaining a $\beta'_{\text{Cs-Rb}}$ 20 times smaller than $\beta'_{\text{Rb-Cs}}$, a result showing the nonreciprocity for β', as discussed before. The observation of such a large difference, much larger than that expected from the mass ratio alone, is a strong indication that other important parameters such as interatomic potentials, or the changes in trap depth, are very important to explain the β' observations. Simple calculations show that all those parameters are able to modify considerably the absolute values (and the behavior) of β'.

As an additional contribution to the large β' value, for heteronuclear collisions the atom pairs come into resonance with the trap lasers at a much smaller internuclear spacing than for the homonuclear case. Therefore in the heteronuclear case, the quasimolecule acquires a large probability to dissociate, undergoing intramultiplet mixing that results in a change of the fine-structure level. The kinetic energy gained in this process by far exceeds the MOT depth and all the fine-structure collisions result in trap losses. However, we do not know the actual FSC contribution to the total heteronuclear trap loss rate.

Notice that the β' values obtained by the two experiments correspond to different MOT parameters and also different Rb isotopes, as presented in Table I. We believe that the different MOT parameters have a small influence on the β' values because of the very large energy gained by the Rb atoms in collision with Cs atoms. On the contrary, for the Rb-Rb collisions, the β values in the range of low trap laser intensities are very sensitive to the MOT parameters, and then it results in considerable differences between the two isotopes. The β dependence on the MOT parameters arises mainly when the small energy gained by the Rb atoms through hyperfine change collisions may be counterbalanced by the MOT trap depth.

The data in Fig. 3 show for a small range a very large change on the absolute β' values at low trap laser intensities. On the other hand, a small variation of β' was observed when the laser intensity was increased. The overall change of β' is roughly one order of magnitude, in agreement with the change measured in other heteronuclear alkali metals [7].

The asymptotic internuclear potentials for heteronuclear ground-excited pairs are not all attractive. For example, the Rb($5P$)-Cs($6S$) potentials are all repulsive because the absolute energy value of the Rb first excited state is larger than that of the Cs atom. The perturbative approach applied to calculate the quasimolecular potentials produces a repulsive R^{-6} interaction for those interacting atoms, as analyzed in detail in Ref. [13]. Therefore, collisions between excited Rb and ground Cs atoms cannot contribute to the trap loss rate because their internuclear distance are not allowed to reach the small values required for the RE and FSC processes to take place. On the other hand, for the case of excited cesium atoms and ground rubidium atoms the attractive interacting potential allows the atoms to reach a short internuclear distance, with an increase of the trap loss rates.

In order to analyze the dependence of β' on the laser intensity, the Rb($5S$)-Cs($6P$) collisions may be considered

as the main loss channel. It may be supposed that the observed increase at low trap laser intensities is associated with the hyperfine change collision mechanism [18]. However, rough calculations with the energy gained during those collisions taken into account show the importance of this mechanism only at intensities lower than the minimum observed in Fig. 3, even if the 9-GHz hyperfine energy difference is supposed to be completely transferred by the Cs atoms to the Rb. In fact, the Rb β loss data of [18] present a minimum at lower intensities. On the other hand, an important role associated with the Cs HCC would support the similar behavior observed for the two isotopes. To understand the trap laser dependence, note that the Cs($6P$) population remains constant when the Rb trap laser intensity changes, and two different mechanisms play a role. The rubidium trap depth decreases with the rubidium trap laser intensity, thus the rubidium atoms escape more easily from a shallow potential. Furthermore, the Rb ground population increases when the Rb trap laser intensity decreases, providing a larger number of Rb($5S$)-Cs($6P$) colliding pairs and therefore an increase of the trap losses since, as explained before, this represents the main loss channel for the crossed species. The combination of both mechanisms, the decrease of the trap depth and the increase of the Rb ground population, produces higher escape probabilities and higher β' values at low laser intensities, below 30 mW/cm^2, Fig. 3. In order to test the relative role of the two processes, we have plotted in Fig. 2(c) β' versus the Rb ground-state fraction Π_{Rb}, calculated as the complement to one of the excited-state fractions whose expression was given in [19]. If the modification in the number of ground-state colliding Rb atoms was the predominant mechanism for β', the data in Fig. 2(c) should show a linear dependence of β' on Π_{Rb}. Although this linear dependence is not evident, then we believe that both the ground-state occupation and the trap depth play an important role. This observation reinforces the above statement that the Brazilian and Italian results should be examined taking into account the different trap depths.

For laser intensities above 60 mW/cm^2 β' still increases but the variation is smaller than that obtained in the low-intensity range. It should be mentioned that other trap loss mechanisms are allowed at high laser intensities, and among those we shall emphasize the two excited atoms channel: Rb($5P$)-Cs($6P$); a similar process has been reported in [6,20]. These additional mechanisms may be important in the complete interpretation of our data.

V. CONCLUSIONS

To summarize, we have measured the heteronuclear trap loss rate for the mixture of trapped ^{85,87}Rb and ^{133}Cs atoms. We have determined as in previous works for the other two-component MOT's [3–9], that the absolute values of β' are larger than those of homonuclear loss rates β for similar experimental conditions. This result is consistent with the mass ratio effect, i.e., the lighter atoms will gain more kinetic energy and escape more easily from the trap. Furthermore, we believe that the increase observed at the low intensity of the rubidium trap laser is associated both with the presence of a shallow trap potential and an increase of the Rb ground-state fraction, i.e., of those atoms contributing to the trap loss collisions. The nonreciprocity of $\beta'_{\mathrm{Cs\text{-}Rb}}$ and $\beta'_{\mathrm{Rb\text{-}Cs}}$ may be related to the mass ratio, the nature of the loss mechanism, the relative values of the attractive potential coefficients, etc.

The present investigation of the inelastic collisions between Rb and Cs cold atoms represents an important step towards a new class of experiments involving binary atomic mixtures. Moreover, the Rb-Cs system, chosen because of its large relative Franck-Condon factor, will bring new perspectives to the heteronuclear photoassociation experiments.

ACKNOWLEDGMENTS

The Brazilian work was supported by FAPESP (Fundação de Amparo à Pesquisa do Estado de São Paulo), Pronex (Programa de Núcleos de Excelência em Optica Básica e Aplicada), and Finep (Financiadora de Estudos e Projetos). The Italian work was supported by the INFM through the PRA on BEC, by the Consiglio Nazionale delle Ricerche through a Progetto Integrato in collaboration with the IFAM of Pisa, and by the MURST. D.W. gratefully acknowledges financial support from the European Union (TMB Contract-Nr. ERBFMRXCT960002).

[1] For early work, see M. Prentiss, A. Cable, J. E. Bjorkholm, S. Chu, E. L. Raab, and D. E. Pritchard, Opt. Lett. **13**, 452 (1988); D. Sesko, T. Walker, C. Monroe, A. Gallagher, and C. Wieman, Phys. Rev. Lett. **63**, 961 (1989); J. Kawanaka, K. Shimizu, H. Takuma, and F. Shimizu, Phys. Rev. A **48**, R883 (1993); L. G. Marcassa, V. S. Bagnato, Y. Wang, C. Tsao, J. Weiner, O. Dulieu, Y. B. Band, and P. S. Julienne, *ibid.* **47**, R4563 (1993).

[2] For a recent review, see J. Weiner, V. S. Bagnato, S. C. Zilio, and P. S. Julienne, Rev. Mod. Phys. **71**, 1 (1999).

[3] W. Süptitz, G. Wokurka, F. Strauch, P. Kohns, and W. Ertmer, Opt. Lett. **19**, 1571 (1994).

[4] W. Scherf, V. Wippel, T. Fritz, D. Gruber, and L. Windholz, Europhys. Conf. Abstr. **22D**, 6 (1998).

[5] M. S. Santos, P. Nussenzveig, L. G. Marcassa, K. Helmerson, J. Flemming, S. C. Zilio, and V. S. Bagnato, Phys. Rev. A **52**, R4340 (1995).

[6] G. D. Telles, L. G. Marcassa, S. R. Muniz, S. G. Miranda, A. Antunes, C. Westbrook, and V. S. Bagnato, Phys. Rev. A **59**, R23 (1999).

[7] J. P. Shaffer, W. Chapulpczak, and N. P. Bigelow, Phys. Rev. Lett. **82**, 1124 (1999); Phys. Rev. A **60**, R3365 (1999).

[8] U. Schlöder, H. Engler, U. Schnemann, R. Grimm, and M. Weidemüller, Eur. Phys. J. D **7**, 331 (1999).

[9] Y. E. Young, R. Ejnisman, J. P. Shaffer, and N. P. Bigelow, Phys. Rev. A **62**, 055403 (2000).

[10] A. Fioretti, J. H. Müller, P. Verkerk, M. Allegrini, E. Arimondo, and P. S. Julienne, Phys. Rev. A **55**, R3999 (1997).
[11] L. G. Marcassa, R. A. S. Zanon, S. Dutta, J. Weiner, O. Dulieu, and V. S. Bagnato, Eur. Phys. J. D **7**, 317 (1999).
[12] J. P. Shaffer, W. Chalupczak, and N. P. Bigelow, Eur. Phys. J. D **7**, 323 (1999).
[13] M. Marinescu and H. R. Sadeghpour, Phys. Rev. A **59**, 390 (1999).
[14] Tin-Lun Ho and V. B. Shenoy, Phys. Rev. Lett. **77**, 3276 (1996); H. Pu and N. P. Bigelow, *ibid.* **80**, 1130 (1998).
[15] H. Wang and W. C. Stwalley, J. Chem. Phys. **108**, 5767 (1998).
[16] The Gaussian waist is defined as the radius at which the atomic density is reduced by a factor $1/e^2$ from the peak density.
[17] D. Hoffmann, P. Feng, and T. Walker, J. Opt. Soc. Am. B **11**, 712 (1994).
[18] S. D. Gensemer, V. Sanchez-Villicana, K. Y. N. Tan, T. T. Grove, and P. L. Gould, Phys. Rev. A **56**, 4055 (1997).
[19] C. Gabbanini, A. Evangelista, S. Gozzini, A. Lucchesini, A. Fioretti, J. H. Müller, M. Colla, and E. Arimondo, Europhys. Lett. **37**, 251 (1997).
[20] L. G. Marcassa, G. D. Telles, S. R. Muniz, and V. S. Bagnato, Phys. Rev. A **63**, 013413 (2001).